PROCEEDINGS, 45th Workshop on Geothermal Reservoir Engineering
Stanford University, Stanford, California, February 10-12, 2020
SGP-TR-216

Geophysical Activities over the Utah FORGE Site at the Outset of Project Phase 3

Philip E. Wannamaker[1], Stuart F. Simmons, John J. Miller, Christian L. Hardwick, Ben A. Erickson, Steve D. Bowman, Stefan M. Kirby, Kurt L. Feigl and Joseph N. Moore

[1]University of Utah/EGI, 423 Wakara Way, Suite 300, Salt Lake City, UT 84108, USA

pewanna@egi.utah.edu

Keywords: Forge, EGS, Geophysics, Seismic reflection, Geodesy, Gravity, Magnetotellurics

ABSTRACT

The Utah Frontier Observatory for Research in Geothermal Energy (FORGE) enters Phase 3 activities with a suite of geophysical observations and models for characterizing the site and providing background properties for upcoming experiments. Reprocessed and migrated seismic reflection results expand the domain of good imagery and show a clear alluvial bedrock interface dipping ~25 degrees westward with a depth that agrees with the well 58-32 intercept at ~3200 feet (975 m). Two-dimensional regularized inversion of gravity data used the bedrock profile as a primary constraint and yielded a model with localized high density below the basement interface nearby to the south of the FORGE site that may represent local dioritic composition. Geodetic GNSS monuments anchored into alluvium over the FORGE site area with bedrock-anchored reference sites display cm-scale possible ground motions in initial processing which may include significant seasonal hydrological effects. Initial InSAR survey scenes suggest similar vertical motion. New tensor magnetotelluric surveying adds 122 sites for testing the overall structural model at several scales and abuts related surveying across the Mineral Mountains and Roosevelt Hot Springs system to the east. Inversion mages from the latter data set show low resistivity lineaments in the upper few km trending just west of north. A low resistivity body in the 4-8 km depth range below the Quaternary rhyolite flows and domes is offered as a possible residual source zone for the eruptives.

1. INTRODUCTION

In 2018, the U.S. Department of Energy selected a location northeast of Milford, Utah, as its Frontier Observatory for Research in Geothermal Energy (FORGE) to develop technology for characterizing and creating Enhanced Geothermal System (EGS) reservoirs (Moore et al., 2019, 2020). Efforts to date have centered around characterization well 58-32 drilled to a depth of 7536 feet (2297 m), including penetration of 4340 feet (1323 m) of granitic basement (Figure 1). This well achieved a temperature of essentially 200 C at total depth as predicted, and showed fracture patterns and stress fields similar to those observed to the east in the Mineral Mountains (Simmons et al., 2019, 2020). Temperature contours dip at a shallow angle westward although details there are subject to minor change as new data arrive. The granitic basement interface is interpreted as a detachment surface accommodating the abrupt unroofing of the Mineral Mountains ~8 Ma (Bartley, 2019). Site characterization is in anticipation of deeper, inclined paired wells aimed at optimizing injection and production strategies for EGS (Moore et al., 2019, 2020).

Because physical properties can influence the state of stress and thermal regime, and may change over the lifetime of FORGE investigations, plus basic uncertainties remain about the overall structural setting, a variety of geophysical methods is being applied in the FORGE area. Reflection seismic data acquired for FORGE have undergone reprocessing for noise removal and extension of domain of reliability, with subsequent prestack depth migration. These are particularly key in establishing the basement-alluvium interface with implications for the stress field. The 3D gravity distribution has been subject to a regularized inversion using the seismically imaged bedrock interface as a geometric constraint. To investigate the efficacy of longer-term ground motion detection, geodetic GNSS stations have been installed with corroboration by Interferometric synthetic aperture radar (InSAR) scene analysis. An extensive magnetotelluric (MT) resistivity survey was acquired over the FORGE property and surrounding area to the clarify structural setting and to provide background resistivity for potential 4D variations in the future.

We specifically do not discuss status of seismicity monitoring and behavior in the FORGE project as that is discussed in Pankow et al (2020). Similarly, we do not touch upon heat flow as this field is incorporated in the overall earth model described by Simmons et al (2020).

2. REPROCESSED SEISMIC REFLECTION STRUCTURES

In November 2017, ~7 mi^2 (~17 km^2) of new 3D multichannel seismic reflection data were acquired through contract over and immediately around the FORGE site (Figure 2). In addition, two legacy 2D seismic lines of 7-8.5 mi (11-14 km) length were acquired from a commercial data broker with limited publication rights. Processing at the time of acquisition revealed a continuous alluvium-granite surface dipping westward and lacking in evidence of subvertical fault offsets beneath the FORGE site (Miller et al., 2018, 2019a; Hardwick et al., 2018, 2019; Simmons et al., 2019). However, processing was not completed for the majority of lines and a significant amount of apparent noise remained in the records. Hence, it was decided to have these seismic data reprocessed using state of the art techniques by Land Seismic Noise Specialists (LSNS) of Denver, Colorado, aimed at refining the seismic interpretation for improved imaging of the valley fill-granite contact, and of the deposits above the granite basement (Miller et al., 2019b). Special

attention was paid to the prestack removal of noise such as ground roll and any other noise identified by testing. In addition, depth imaging (migration) was performed.

Details of the acquisition parameters and data CDP binning for the reflection data are described in Miller et al (2018, 2019). One key determinant of image quality is seismic fold. Edge effects arise when the common depth point (CDP) binning is too restricted to contain a large distribution of source-receiver offsets, thus offering poor velocity interrogation and resolution. Inspection of both migrated and unmigrated time images indicates that sufficiently high fold was obtained to a distance of ~1.5 km west and ~1 km east of FORGE well 58-32 (Miller, 2019). Especially toward the east end of the survey, particularly for the long 2D line 302 (Figure 2), application of refraction statics was necessary but revealed that the shallow bedrock interface was flat with no local basins. The velocity model determined directly from the seismic data was highly azimuth-dependent, meaning the velocity field changed depending on the azimuth between the source and receiver (horizontal anisotropy). It is surmised from this anisotropy that there was non-uniform sedimentation processes during basin evolution, but this cannot be stated conclusively without additional well data.

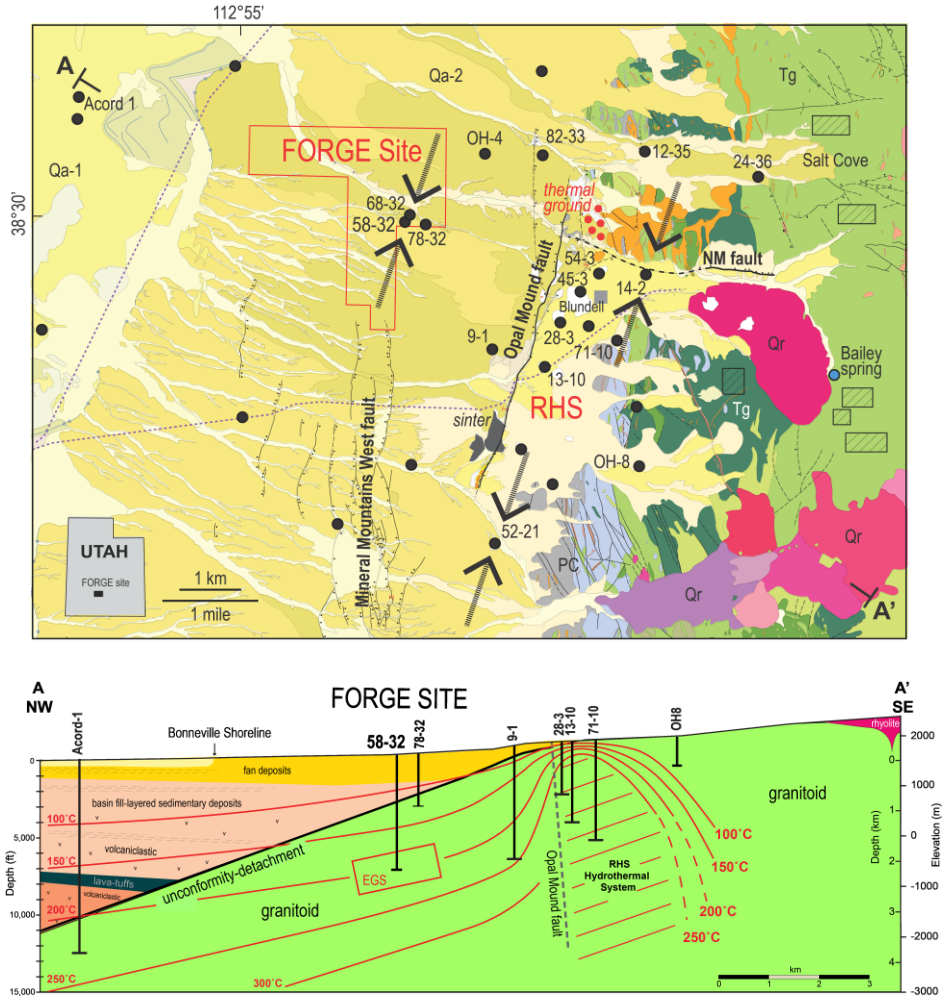

Figure 1: Idealized geological map and cross section for the Utah FORGE site after Simmons et al (2019). Abbreviations: QA-1 = Lake Bonneville silts and sands; QA-2 = alluvial fan deposits Qr = Quaternary rhyolite lava and pyroclastic deposits; T = Tertiary granitoid; PC = Precambrian gneiss; and black-filled circles – wells. Thermal contours subject to refinement with further data.

Both prestack time and depth migration were performed. Unmigrated and migrated time images alike show a continuous basement reflector dipping to the west, plus near-horizontal presumed sedimentary structures in the alluvium (Figure 3a,b) (Miller, 2019). A migration algorithm that used an estimated anisotropy parameter in the vertical direction (parameter delta) was shown to migrate the depth of the granite interface on the seismic data to that of well 58-32 (Figure 3c,d). Another indication of vertical offset would be diffracted energy in the unmigrated version (Figure 3a) and no diffractions are observed. The prestack depth migration of line IL-93 using the estimated anisotropic migration again shows the top of granite reflection is interpreted to be continuous (Figure 3c). The depth at well 58-32 is indicated by the horizontal amber line in Figure 3d. The question of how much vertical offset in the top-of-granite surface can be detected using the reflection seismic method can be answered using the ¼ wavelength principle (Yilmaz, 2001), which is a function of the recording process and the earth properties. This principle states that the minimum offset that can be detected is approximately ¼ of the dominant frequency of the seismic wavelet. In this survey, the dominant frequency of the data is 30 Hz (f) and the velocity immediately above the top of granite is 3000 m/s (v). Therefore, the wavelength, v/f, is 100 m. So, using the ¼ wavelength

principle we can expect to detect offsets in the granite reflector of 25m or greater. The quasi-horizontal nature of sediment interfaces in the alluvium implies that the interface is not a continuous growth fault but rather was established relatively abruptly ~8 Ma (Bartley, 2019). Vertical offset within 25 m over such a time span implies a low faulting hazard potential.

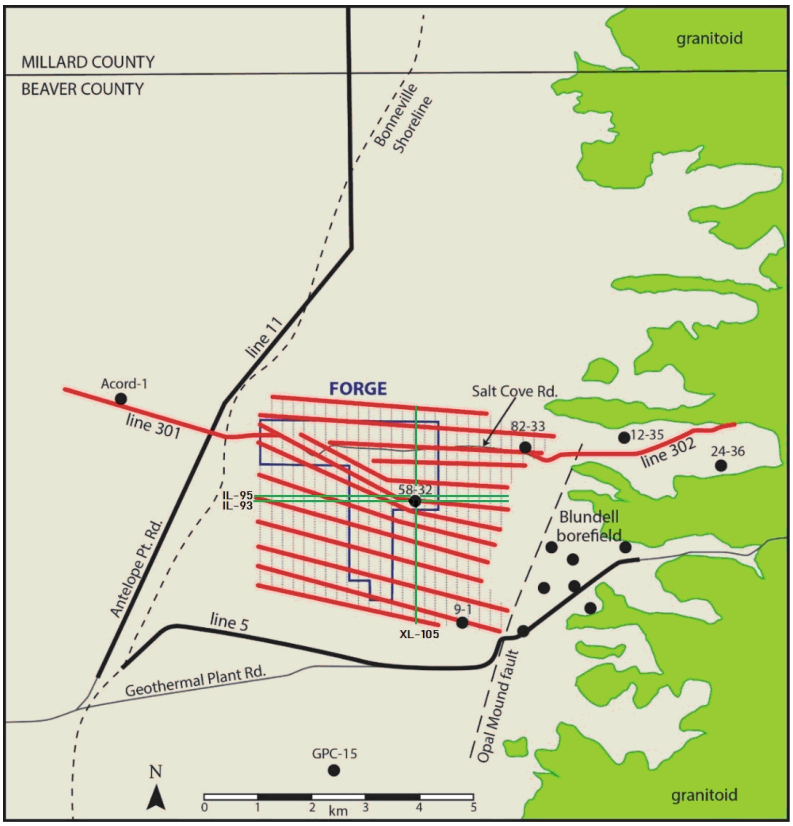

Figure 2: Reflection seismic survey profile locations over the FORGE area (Miller et al., 2018, 2019). The 3D survey area comprises 13 red source lines (vibrator point locations 50 m apart), and 27 gray geophone lines geophone locations (oriented N-S, geophone interval 50 m). Red lines 301 and 302 are new 2D seismic lines; heavy black lines labeled 5 and 11 are legacy 2D lines licensed from Seismic Exchange, Inc. Green lines are 3D inlines (IL) and crosslines (XL) discussed herein.

Views along strike (~N-S) are revealing of modest basement interface topography. The characterization well 58-32 appears to lie in a gentle, local depression of the alluvium-bedrock interface (Figure 4). This is confirmed by reprocessing of legacy line 11 in Figure 2 (Miller, 2019). The northern edge of the depression, if projected straight eastward, approximately coincides with Negro Mag Wash. Sediment infill appears local, with continuous layering from the flanking basement interface upward. This suggests the depression existed essentially at the same time as abrupt unroofing of the Mineral Mountains along the detachment ~8 Ma and was quickly filled.

3. 3D GRAVITY INVERSE MODELING AND 4D BASELINE

Basin-wide gravity data and modeling over the FORGE and surrounding area during Phase 2 of the project is described in detail by Hardwick et al (2018, 2019). Data and 2D modeling of gravity profiles is compatible with a steadily westward dipping alluvium-basement interface to a maximal depth west of the center of Milford Valley. To complete Phase 2C activities, additional survey densification was completed over a ~8 x 5 km grid largely centered upon the FORGE footprint (Figure 5). These stations served as inputs to a 3D density model using regularized inversion carried out for the Utah Geological Survey by Witter (2019). In such inversions, the earth subsurface domain is discretized into many cells or voxels whose density is sought to fit the gravity data while simultaneously preserving model stability through lateral spatial smoothing following the method of Fournier and Oldenburg (2019). Cell sizes in the center area of the model were 50h x 50w x 30d meters, thickening toward the deeper parts of the model, with topography included. A fundamental constraint of the inversion was imposition of the alluvium-bedrock interface with average starting density values of 2.42 gm/cc for alluvium and 2.65 gm/cc for the bedrock (Witter, 2019).

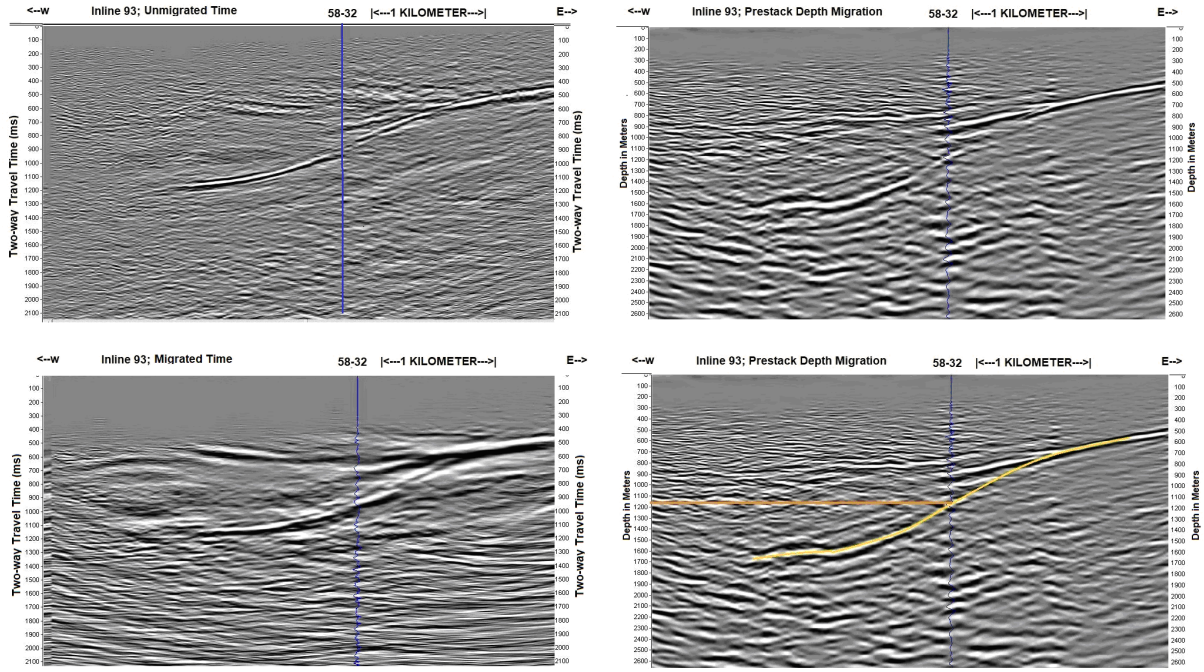

Figure 3: Top left (a), Unmigrated Time processing for line IL-93 passing through well 58-32; Bottom left (b), Migrated time version of top, showing a horizontally continuous reflection from the top of the granite with no significant vertical offset. The location of test well 58-32 is shown in blue; Top right (c), Uninterpreted estimated anisotropic prestack depth migration; Bottom right (d), Interpreted version of the top. Yellow line indicates the author's interpretation of the top of granite reflector. The horizontal amber line indicates the depth to top-of-granite at well 58-32.

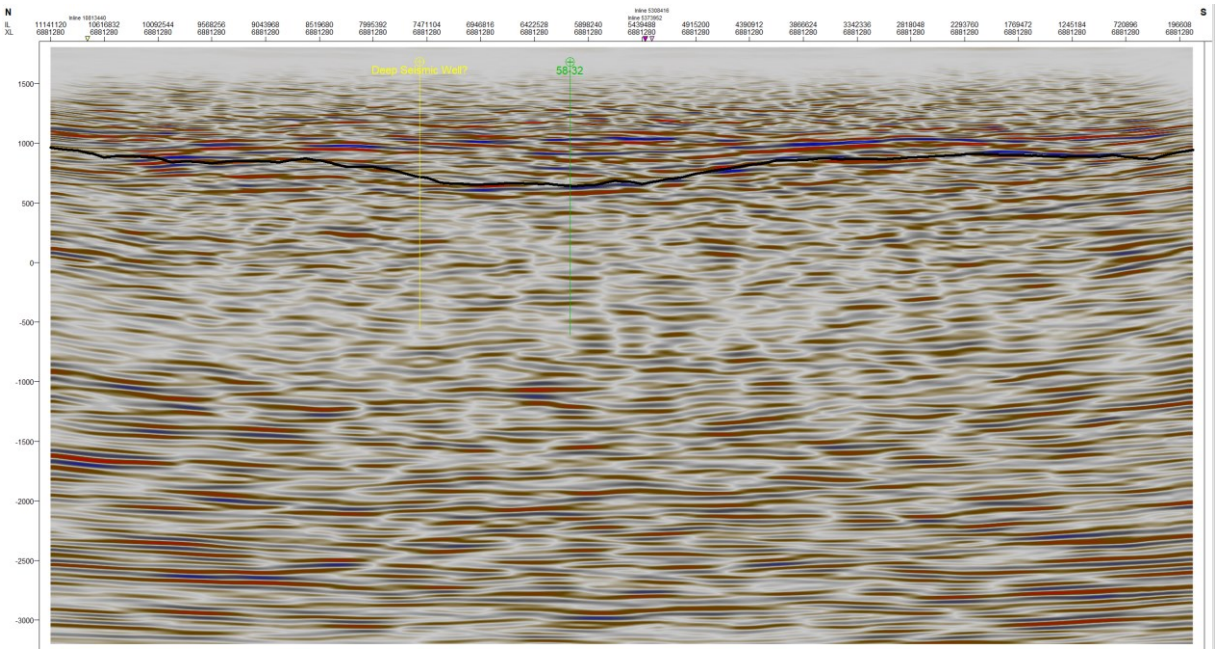

Figure 4: North to south depth migrated seismic section through well 58-32 with interpreted basement contact. Well 58-32 is shown in green and possible additional seismic monitoring well is shown in yellow.

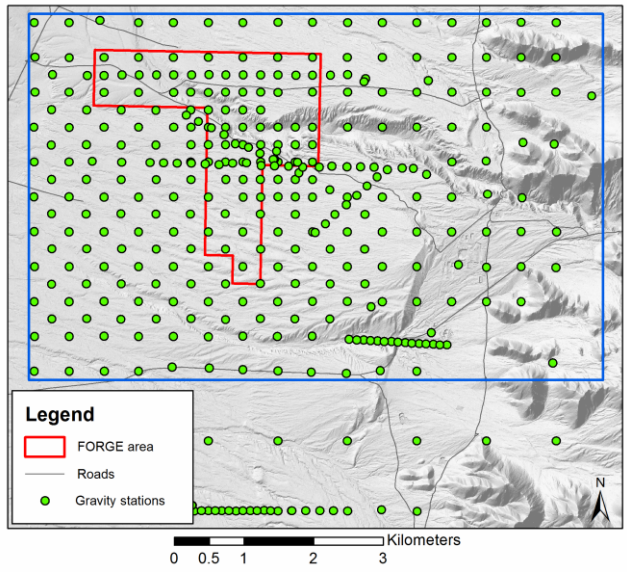

Figure 5: Map of newly acquired gravity stations over the FORGE site area for 3D inversions analysis.

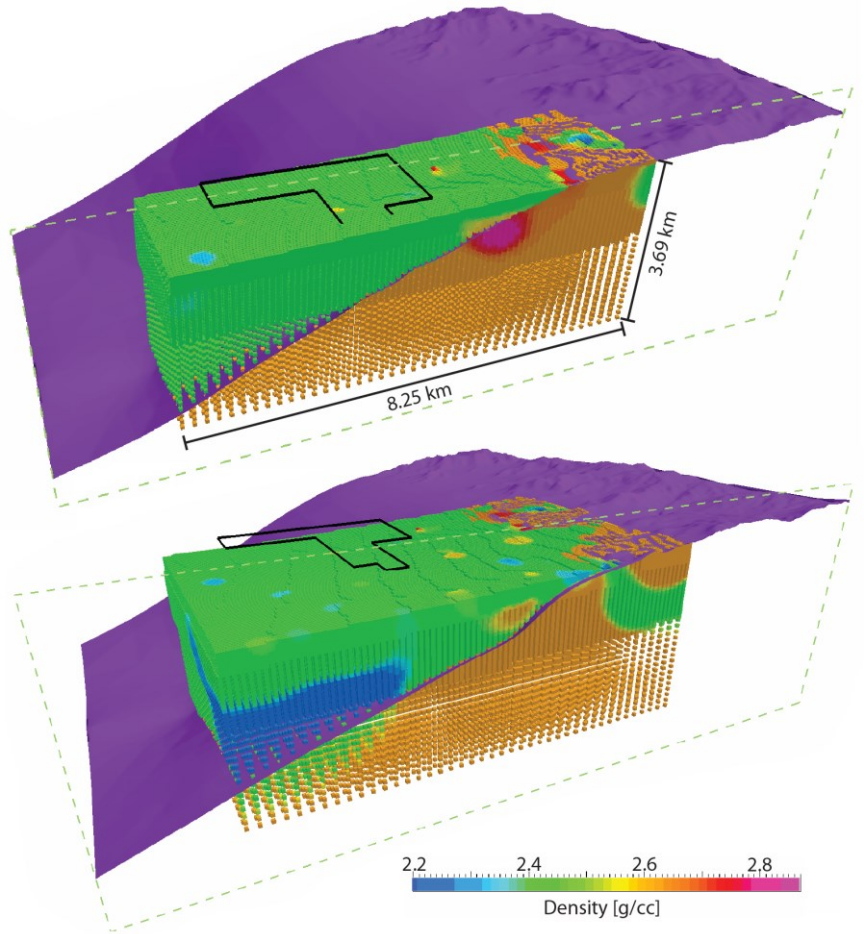

Figure 6: East-west density cross sections from 3D regularized inversion of gravity data over the FORGE site. Modified from Hardwick and Hurlbut (2019) after Witter (2019).

A good fit to the gravity data assuming a tight error floor of 0.03 mgal (Witter, 2019) and example cross sections from the inversion study appear in Figure 6. Gravity modeling experiences strong non-uniqueness and so the basement interface constraint is key. In the upper Figure 6 section close to the FORGE site, adherence to a steadily dipping interface yields a localized high-density feature in the shallowest basement correlated with local diorite rich volumes in the granitic basement. There is a slight 'leakage' of the high density

into the deeper alluvium above but this likely is an artifact of the smoothing regularization. A subtle gravity gradient anomaly trending SE-NW along the SW edge of the FORGE site depicted in Hardwick et al (2019) appears to be unfounded based on the new data sampling. In the lower cross section of Figure 6, the main new feature is a tabular low-density zone in the deep alluvium southwest of the FORGE site. Basement depth is less well known farther from the FORGE footprint and, if deeper than assumed, could explain part of the anomaly. Regional gravity trends appear weak in the area, so little influence on this low density is expected.

A 4D gravity survey (i.e., microgravity) was planned and initial measurements carried out for the purpose of benchmarking surface and subsurface elevations and density prior to Phase 3 stimulations. Locations of the microgravity stations (Figure 7) are collocated with GNSS deformation benchmarks (discussed next) and use the same location survey data. The new 4D gravity survey will also be used to further constrain the location of the granite surface and characterize any seasonal variance if it exists in the study area. The microgravity stations were occupied 3 times in conjunction with the GNSS deformation campaigns and preliminary processing was performed to help establish a stable baseline for the monitoring network. The 4D gravity surveys will be combined with changes in the groundwater elevation to assess possible elevation changes measured by GNSS benchmarks and InSAR data.

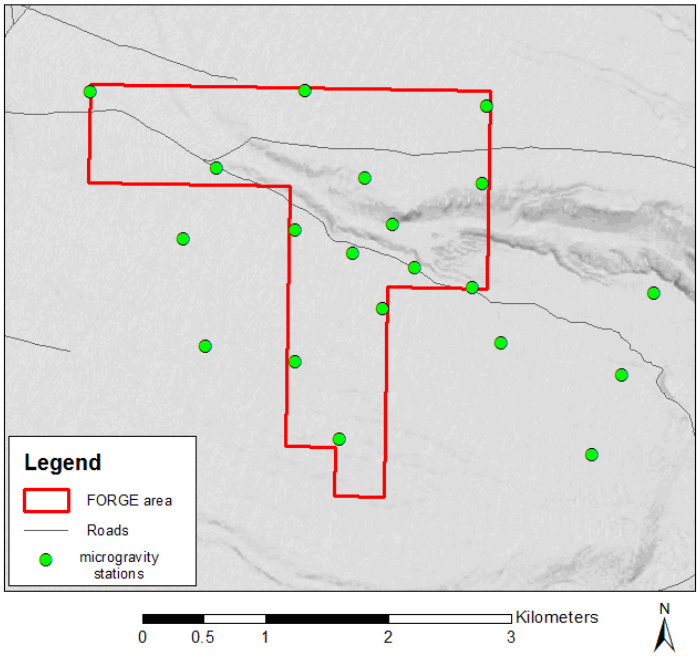

Figure 7: Map of microgravity stations in the FORGE study area, from Hardwick and Hurlbut (2019).

4. GEODETIC GPS AND INSAR MONITORING

Twenty precision GNSS monuments were established in the FORGE area to provide a baseline for ground deformation monitoring during the drilling and stimulation of the deep production/injection wells, and to capture any additional unspecified deformational phenomena (Erickson et al., 2019). In addition to applicability to the FORGE project directly, the network considers infrastructure sensitive to ground deformation, such as the existing PacifiCorp Blundell geothermal plant and the SunEdison-TerraForm Power Milford Flat wind farm. The locations of these are exactly coincident with the gravity stations in Figure 7. Geophysical deformation monitoring stations (GDM-1 to GDM-20) were designed using National Geodetic Survey (NGS) three-dimensional rod monument specifications (Federal Geodetic Control Committee, 1988) for installation in alluvium in order to create a highly stable point from which to measure potential horizontal and/or vertical ground deformation. Station monument stability is greatly improved with the use of a floating plastic sleeve around the upper three feet of the monument rod, decoupling the rod from the near-ground surface. A schematic picture of the monument and field pictures of installation appear in Figure 8 (Erickson et al., 2019). Attention was paid to reducing both discrete and continuous errors due to sources such as topography, vegetation, object multipath, ground freezing, satellite configuration, geomagnetic conditions and atmospheric conditions. Two fixed base stations on granitic bedrock also were established ~5 km east and ~20 km west of the FORGE area as references for time series processing.

The GNSS satellite data were recorded using four Trimble R8 and one R10 receivers sequentially over the 20 monuments and processed with Trimble-provided software to obtain least-squares reduction-derived locations for the monuments during several field campaigns. At the time of this writing, campaigns were conducted in 2018 during middle March, June, November and December. Two example motion solutions for cumulative movement between campaigns are shown in Figures 9 and 10 for March-June and June-November. At many of the sites, computed motions between campaigns are of cm-scale, although error bars commonly compare in amplitude to the motion estimate. Nevertheless, such errors are considered with the normal range for campaign-style, static survey methods (Erickson et al., 2019). For March-June, the vectors are somewhat variable but have a general southward trend (Figure 9). For June-November, the vectors are clearly WSW (Figure 10). Possible causes of motions such as these appear to represent could include hydrological effects,

particularly seasonal ones. To help resolve causes, it will be useful to compare inferred geodetic motions with 4D gravity to corroborate temporal trends. Experience with motions trends over these time scales in the literature are scant; Ji and Herring (2012) show correlation of year-length horizontal motion in the 1-3 cm range on the flanks of the San Gabriel Valley, southern California with well water level including discrete flooding events. Continuation of the GNSS campaign sampled at least quarterly will seek seasonal and other environmental temporal factors.

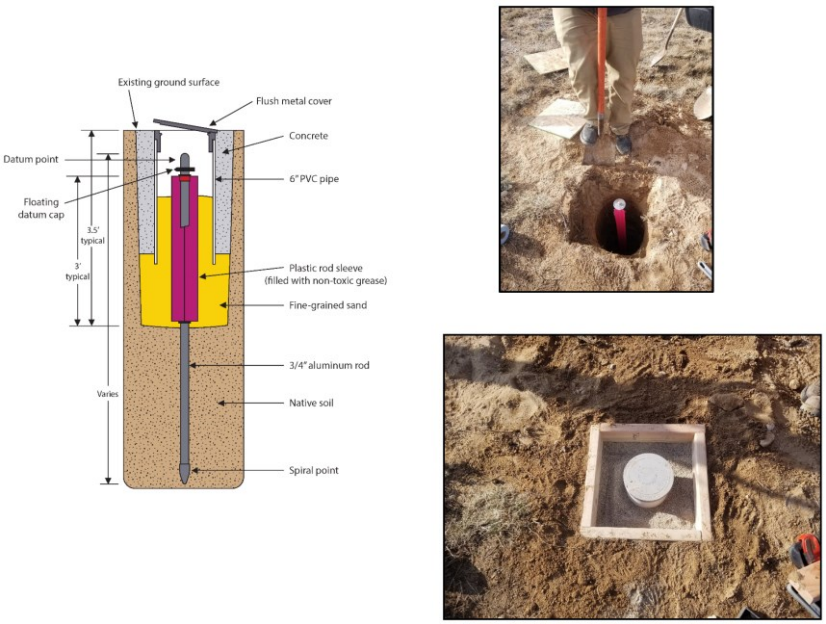

Figure 8: Left: Schematic diagram of ground deformation monitoring station. Right: Pictures of field installation of monitoring station.

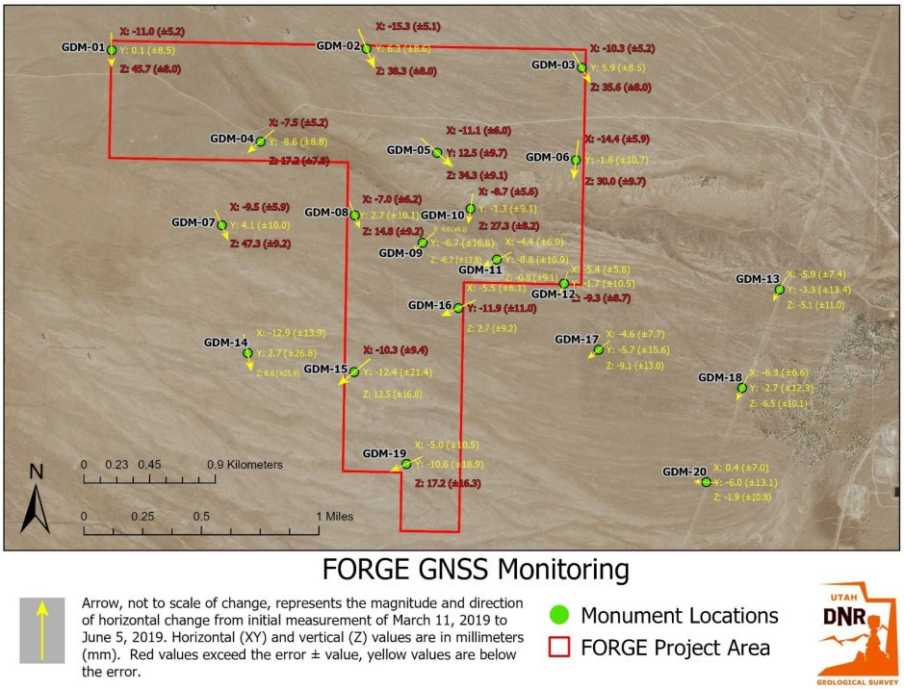

Figure 9: Vector map of monument movements from March 11, 2019, to June 5, 2019, over the FORGE area (from Erickson et al., 2019). Values in red are considered significant with respect to their estimation errors.

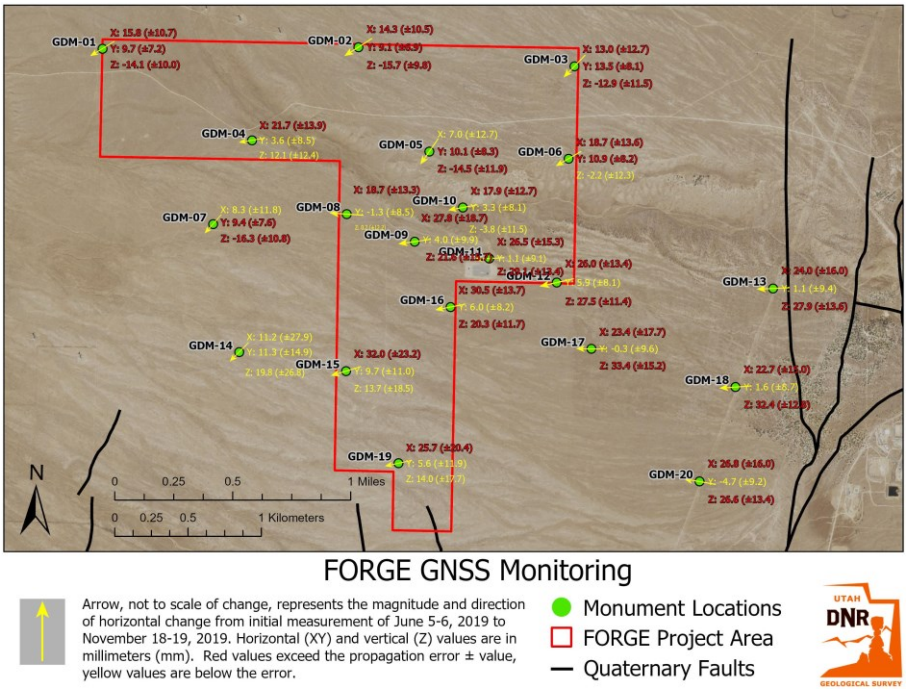

Figure 10: Vector map of monument movements from June 5, 2019, to November 18, 2019, over the FORGE area (B. Erickson, pers. comm., 2020). Values in red are considered significant with respect to their estimation errors.

To quantify the deformation at the Utah FORGE site, we also use Interferometric Synthetic Aperture Radar (InSAR). Since the rate of deformation at the Milford FORGE site in Utah is expected to be low, a careful analysis using many SAR images acquired over several years is required to quantify any deformation at the level of several millimeters per year. To do so, we have analyzed the SAR data from from 2016 to 2019. This data set consists of SAR images acquired by TerraSAR-X and TanDEM-X satellite missions operated by the German Space Agency (DLR) as described by Pitz and Miller (2010).

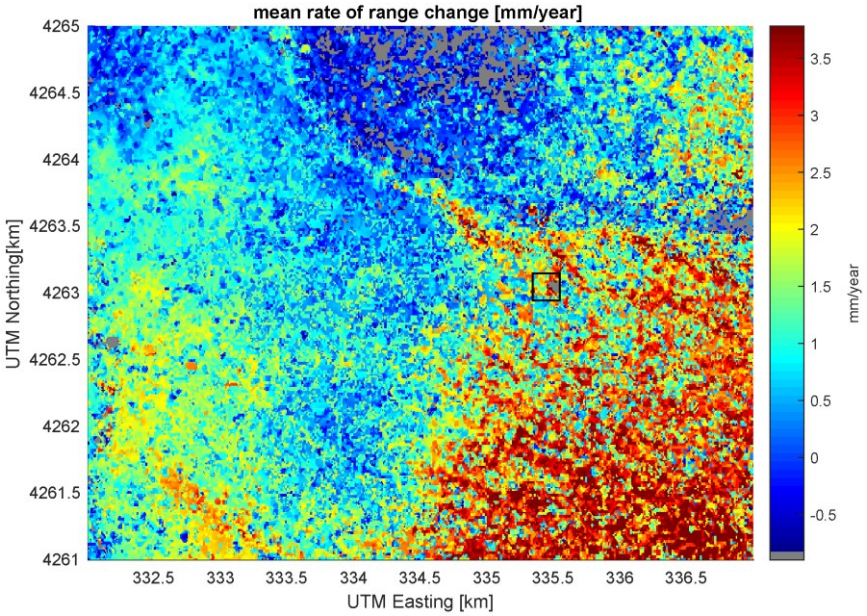

Figure 11: Mean rate of range change in mm/year for stack of interferograms spanning the time interval from 08-Nov-2016 to 01-Jun-2019. Coordinates are UTM (zone 12) easting and northing in km. The black square denotes location of deep well 58-32. Gray areas indicate locations with poor correlation and/or areas where phase could not be unwrapped to calculate the range change. The unit vector pointing from the target on the ground toward the radar sensor aboard the orbiting TerraSAR-X satellite is [E, N, U] = [–0.4160, –0.0812, 0.9055] which is assumed to be constant over the scene and through time.

Interferometric image pairs are acquired from individual dates (Feigl et al., 2019), with the resulting interferograms registered onto the SRTM 3DEP (1/3 arc-second) digital elevation model (DEM). The mean rate of range change measured by InSAR is mapped into UTM coordinates in Figure 11. Little deformation is inferred near the location of deep well 58-32 (square box). This data set has been published on the Geothermal Data Repository with the title, "Utah FORGE: InSAR Data" http://gdr.openei.org/submissions/1154. To address the possibility that the temporal evolution of the deformation field is a seasonal signal with a negligible mean, we plan precise comparisons of GNSS and InSAR data collected at regular intervals over each year during Phase 3 of the FORGE project.

5. MAGNETOTELLURIC BASELINE MEASUREMENTS OVER THE FORGE AREA

New, high-quality, tensor MT data at 122 sites including the vertical magnetic field and utilizing ultra-remote referencing has been acquired over the FORGE project area (Figure 12). The FORGE MT data coverage abuts existing MT coverage of the EGI SubTER MT/ZTEM project over the Mineral Range and Roosevelt Hot Springs to the east. The results will be used to: 1), Delineate the densities of faults and fractures in crystalline basement rocks so that they can be compared to independent data acquired from drilling, geologic field mapping, seismic reflection and gravity surveys and to properties in the Mineral Range; and 2), Derive baseline 3D resistivity structure for later MT monitoring of temporal changes in resistivity structure following well stimulation, which aim to quantify the total volume of stimulated reservoir rock and assist in locating possible fluid connections and flow paths through the fracture mesh in FORGE Phase 3. Based on similar survey geometries in the Habanero well area of the Cooper Basin, Australia (Peacock et al., 2016), peak MT response changes should be in the 0.1-10 s period range (midband). It was decided that near-optimal and practical MT site spacing was of order 0.5 km at the surface over the immediate FORGE area for fracturing target zones at depths of ~2 km.

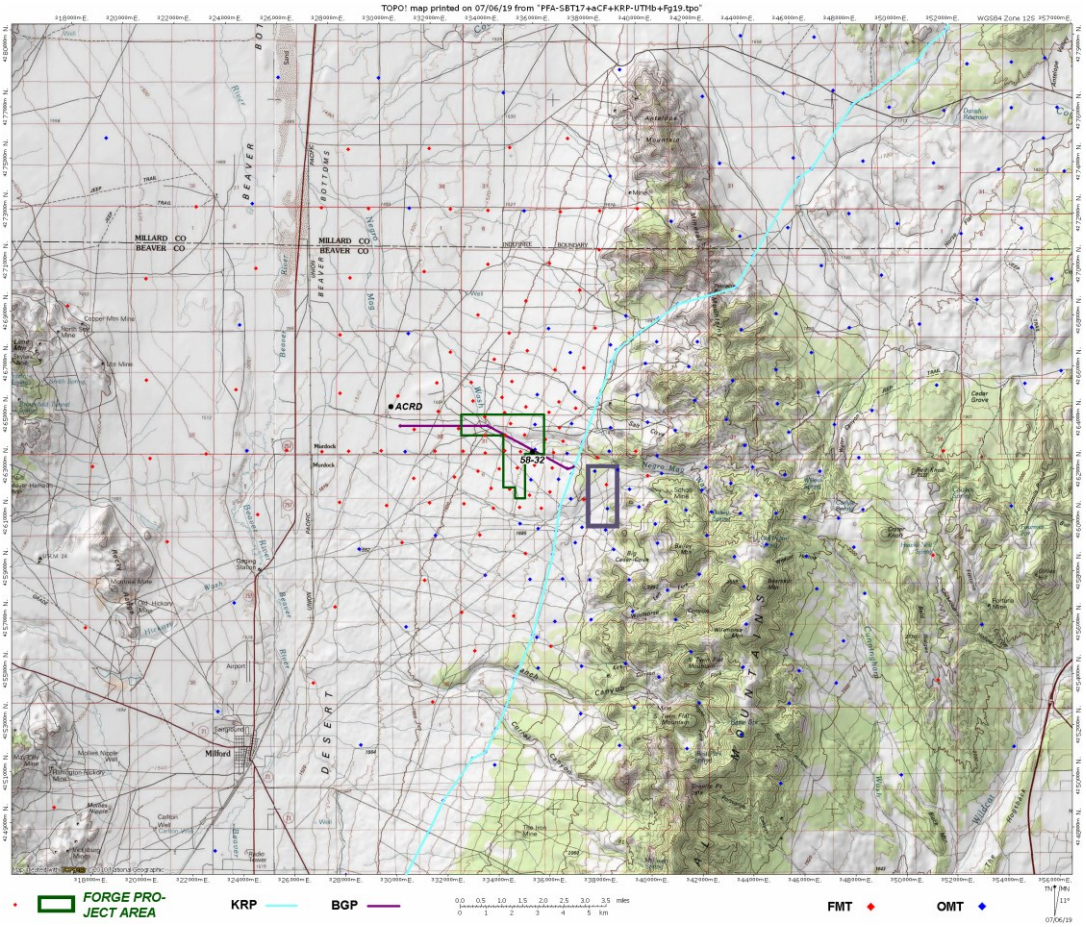

Figure 12: MT survey topographic map of the Utah-FORGE project area showing prior other (blue, OMT) and new station coverage (red, FMT). Cyan trend running NNE-SSW through the project area is the Kern River pipeline (KRP), while shorter E-W proposed biogas pipeline is in purple (BGP). FORGE property boundary as dark green right polygon, and Acord-1 and FORGE test drill site (FDST) wells are marked as black circles. Dark grey rectangle shows approximate production area of the Roosevelt Hot Springs (RHS) geothermal system.

The data were acquired via contractor (Quantec Geoscience LLC) and overall appear to be of very good to excellent quality. Two example soundings appear in Figure 13 which straddle FORGE well 58-32 by 1-2 km each side east-west. Use of an ultra-remote MT reference in western Nevada helped improve midband data quality where cultural and geothermal field noise was especially strong (cf., Wannamaker et al., 2004). Final site distribution was intended to adequately sample the immediate FORGE vicinity plus provide some valley and range scale structural insights for comparison to structural geology and gravity interpretations.

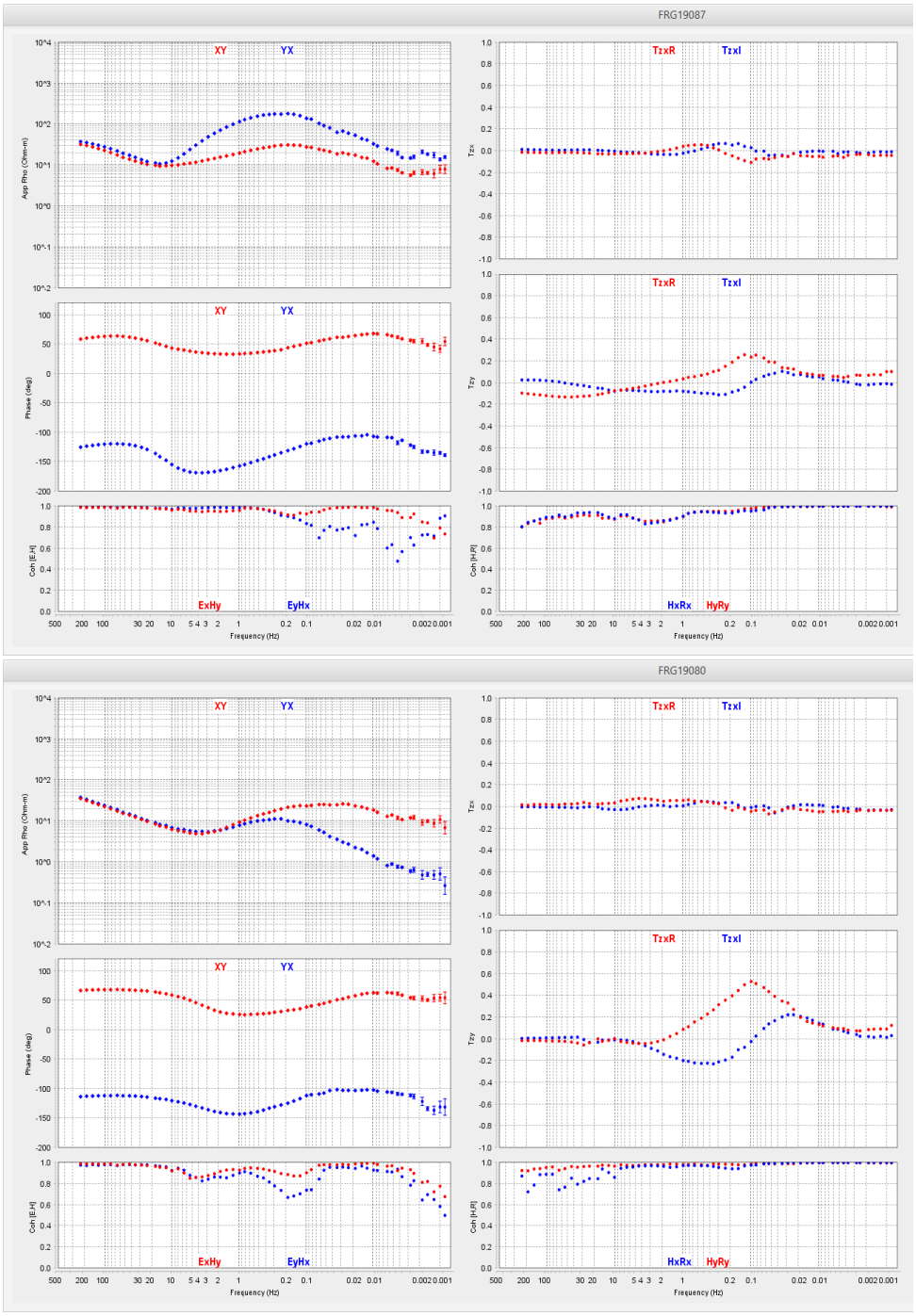

Figure 13: Two example sounding curves from the recently completed FORGE MT survey that straddle well 58-32 by 1-2 km. Upper site (FRG19087) is from the eastern portion of the project area, while lower site (FRG19080) is from the central portion of the area.

A wireframe view of the finite element mesh being utilized for inversion imaging is plotted in Figure 14. Inversion is computed using the algorithm of Kordy et al (2016a,b) developed in-house that utilizes all direct solvers for the model parameter step and can precisely simulate the sometimes steep topography of the area using deformable hexahedral elements. This particular mesh also is deformed horizontally to precisely follow the pathway of the Kern River pipeline whose response is present in the MT data within ~2 km of it. The algorithm runs parallelized on large-RAM (0.5 TB) multicore (e.g., 24) server class workstations. Other example applications of this algorithm have been in integrative geothermal Play Fairway Analysis (Wannamaker et al., 2017, 2019). To date only the pre-existing subset of stations over the Mineral Mountains and Roosevelt Hot Springs to the east of the FORGE site, plus sparse sites over the FORGE area, have been inverted. However, the model from those alone exemplifies the potential of the larger data set. A representative plan view and a cross section are plotted in Figures 15 and 16.

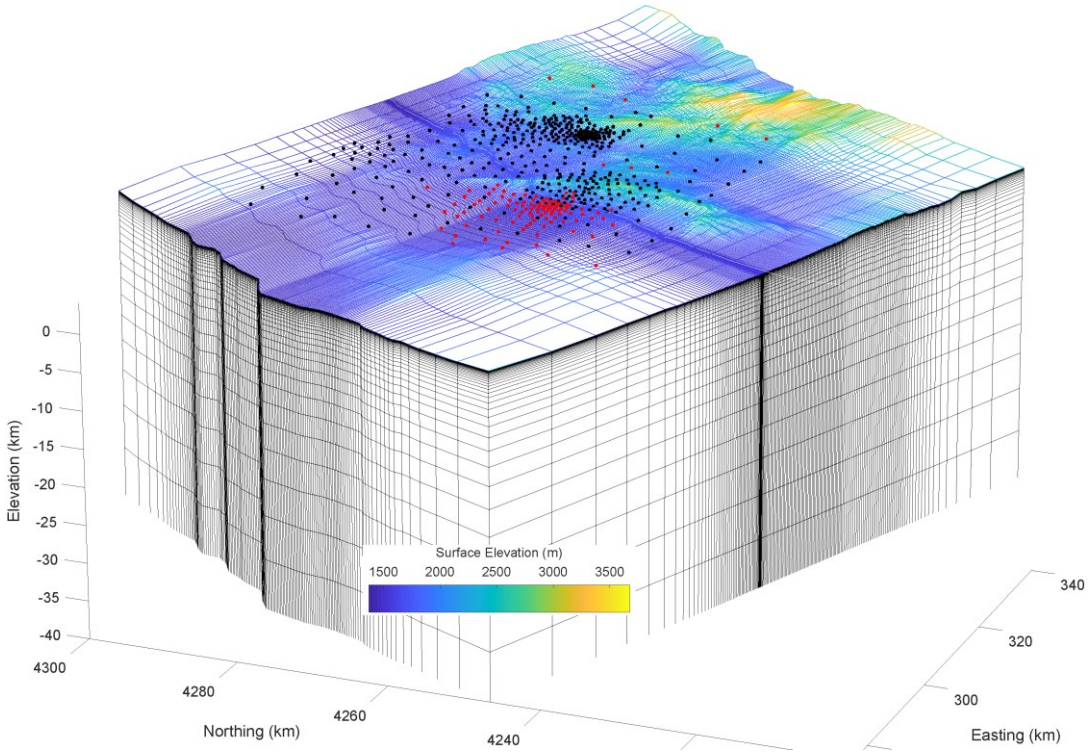

Figure 14: Finite element mesh representation of earth resistivity model for the combined FORGE-SubTER-Cove Fort MT data set (red, black). Red sites are new for the FORGE project, while black sites are pre-existing from Play Fairway Analysis projects of donated by ENEL Corp (Cove Fort). Thin white line trending ~N020 is Kern River pipeline. This file is input to our 3D non-linear inversion algorithm (Kordy et al., 2016a,b). Horizontal units are NAD84 UTM Zone 12S.

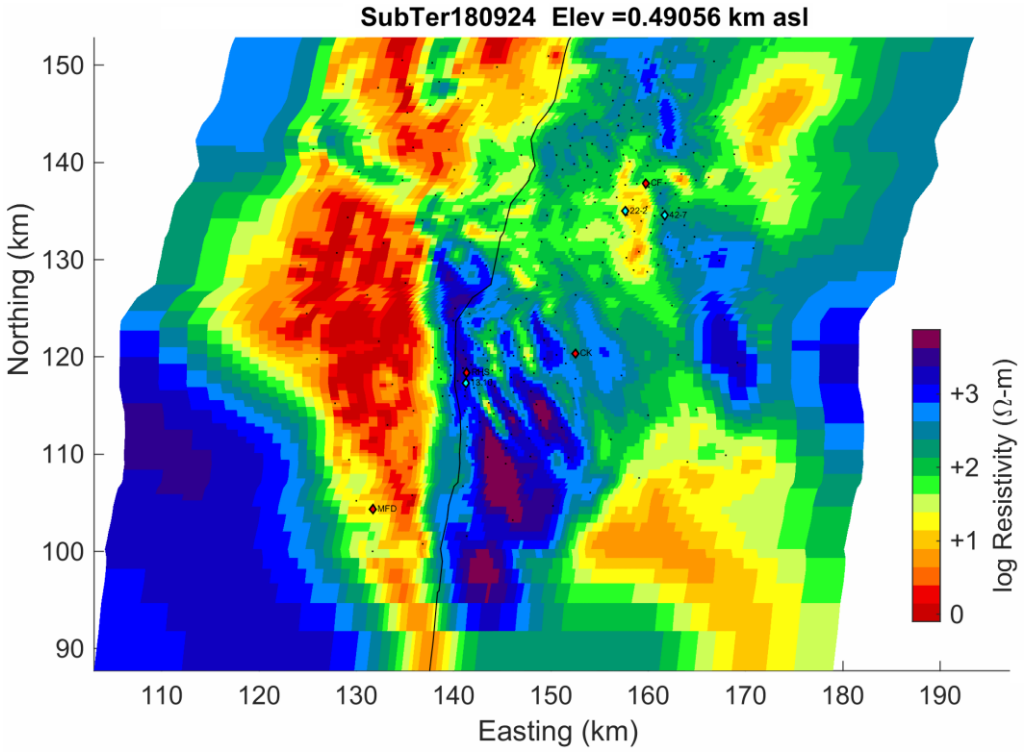

Figure 15: Plan view of MT inversion model using the Mineral Mountains and sparse FORGE sites at ~0.5 km elevation (~1 km depth). Select locations as red diamonds include Roosevelt Hot Springs (RHS), historic Cove Fort (CF) and Milford city (MFD). Coordinates are local mesh, so view would need to be rotated 20 deg clockwise to trend with true north up.

Figure 15 shows several interesting features including a sharp demarcation of the alluvium-bedrock interface at ~1 km depth beneath the FORGE area west of the Kern River pipeline trace. This interface will be mapped with much great precision still when the new FORGE sites are integrated. Over the Mineral Mountains to the east of FORGE and the pipeline trace, three pronounce low resistivity lineaments trending essentially north-south are imaged in the upper km. These are taken as altered fracture zones corresponding to mapped fault trends (Simmons et al., 2019). One of these projects directly into the Roosevelt Hot Springs producing area and may exert control on fault zone permeability there.

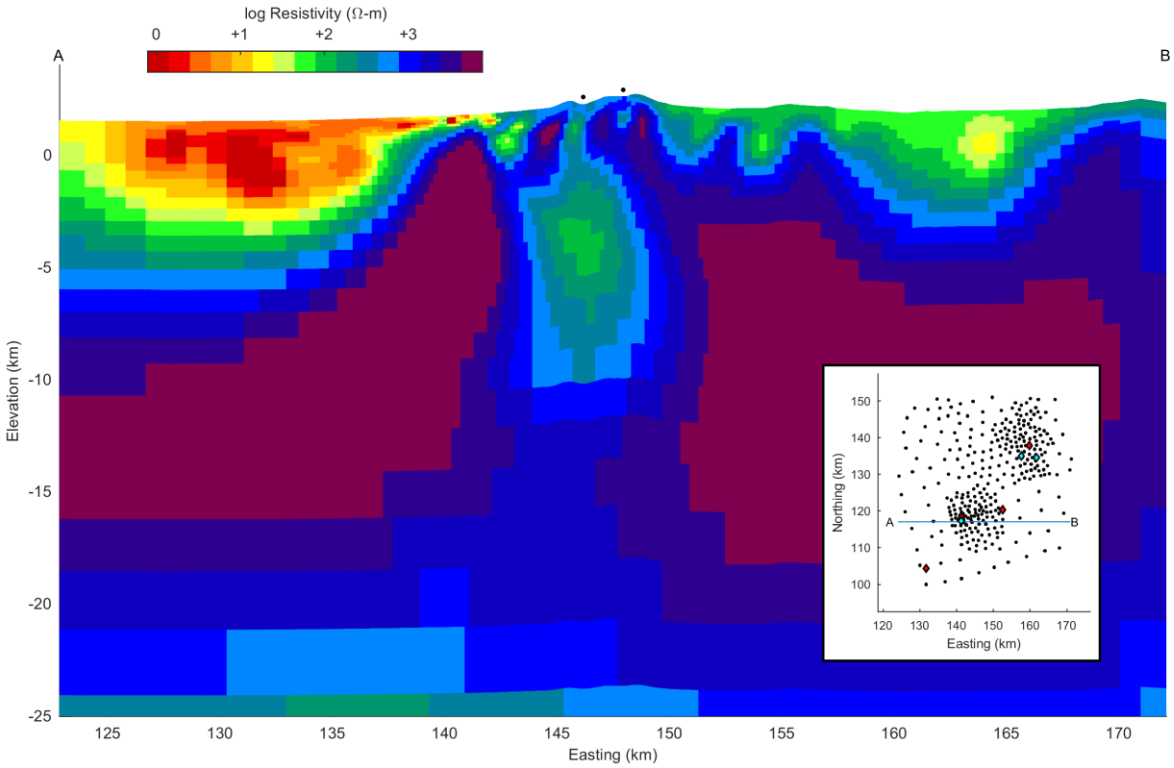

Figure 16: Section view of MT inversion model using the Mineral Mountains and sparse FORGE sites at ~0.5 km elevation (~1 km depth). Select locations as red diamonds include Roosevelt Hot Springs (RHS), historic Cove Fort (CF) and Milford town (MFD). Coordinates are local mesh, so view would need to be rotated 20 deg clockwise to trend with true north up.

Figure 16 is a fascinating cross section in that it appears to show a lower resistivity body in the 4-8 km depth range below the Quaternary rhyolite domes of the Mineral Mountains (Figure 1). This is an appropriate depth for the (possibly cooled) magma storage zone of these rhyolites. The resistivity is not very low, only ~100 ohm-m, although a more compact body of higher contrast presumably could provide an equivalent MT response. The volume instead may represent a fracture zone of residual high-temperature fluids that could contribute to the Roosevelt Hot Springs. The shallower fracture zones pointed out with Figure 15 are seen at high levels over the possible magma chamber volume. The sparse data coverage west of the Roosevelt Hot Springs is already allowing a decent view of the alluvium bedrock interface of eastern Milford Valley beneath the FORGE project area, and this will sharpen substantially with addition of the new MT data. We also will seek whether fracture zones such as imaged in the western and central Mineral Range may exist below the FORGE area, although low permeability as implied by logging of well 58-32 (Moore et al., 2019, 2020) makes this less likely.

6. CONCLUSIONS

Geophysics can allow inferences about the third dimension of geothermal systems unobtainable by other means except drilling. At Utah FORGE, key parameters of interest include the geometry of the alluvium-basement interface, density and orientation of fracture zones in the granitic basement, and possible sources of heat for the system. Seismic reflection data generally image the interface as being sharp and are able to predict its disposition over a range 3-4 km roughly centered on characterization well 58-32. With the basement interface geometry constrained, density variations within either the alluvium or basement are imaged in 3D gravity analysis some of which can be ground-truthed by sampled lithology. Initial ground deformation studies suggest substantial seasonal signals may exist, and ongoing FORGE monitoring will compare GNSS, InSAR and 4D microgravity data variations. MT data so far appear to hold the potential for detection of fracture zones in the granitic basement and are glimpsing potential deep heat source zones below Quaternary rhyolitic volcanic centers.

7. ACKNOWLEDGEMENTS

Research was partially supported by the U.S. Department of Energy under contracts DE-EE0007080 to J. Moore and 7697 to P. Wannamaker. Development of the 3D MT inversion algorithm was supported by contract DE-EE0002750 to P. Wannamaker.

Wannamaker thanks Dr. V. Maris for computation of the 3D MT inversion models on the large-RAM workstations. Synthetic Aperture Radar data from the TerraSAR-X and the TanDEM-X satellite missions operated by the German Space Agency (DLR) were used under the terms and conditions of Research Project RES1236.

REFERENCES

Bartley, J.M.: Joint patterns in the Mineral Mountains intrusive complex and their roles in subsequent deformation and magmatism, *Utah Geological Survey Miscellaneous Publication*, 169-F, 15 pp. (2019).

Erickson, B.A., Bowman, S.D., and Hiscock, A.I.: Utah FORGE observatory for research in geothermal energy (FORGE) project - Phase 2C: Ground deformation monitoring, *Utah FORGE Miscellaneous Report*, September 11, 88 pp. (2019).

Federal Geodetic Control Committee: Geometric geodetic accuracy standards and specifications for using GPS relative positioning techniques, *Federal Geodetic Control Committee report*, 48 pp. (1988).

Feigl, K.L., Thurber, C., Powell, L., Sobol, P., Masters, A., Reinisch, E.C., and Ali, S.T.: General inversion of phase technique (GIPhT), *Github software repository*, https://github.com/feigl/gipht (2019).

Fournier, D., and Oldenburg, D.W.: Inversion using spatially variable mixed Lp norms, *Geophysical Journal International*, 218, 268-282 (2019).

Hardwick, C., and Hurlbut, W.: FORGE Phase 2C activities summary – gravity and temperature logging, *Utah FORGE Miscellaneous Report*, 9 pp. (2019).

Hardwick, C., Hurlbut, W., and Gwynn, M.: Geophysical surveys of the Milford, Utah, FORGE site—gravity and TEM, *in* Allis, R., and Moore, J.N., editors, Geothermal characteristics of the Roosevelt Hot Springs system and adjacent FORGE EGS site, Milford, Utah, Utah *Geological Survey Miscellaneous Publication*, 169-F, 15 pp. (2019).

Ji, K.H., and Herring, T.A.: Correlation between changes in groundwater levels and surface deformation from GPS measurements in the San Gabriel Valley, California, *Geophysical Research Letters*, 39, L01301, 5 pp. (2012).

Kordy, M.A., Wannamaker, P.E., Maris V., Cherkaev, E., and Hill, G.J.: Three-dimensional magnetotelluric inversion using deformed hexahedral edge finite elements and direct solvers parallelized on SMP computers, Part I: forward problem and parameter jacobians, Geophysical Journal International, 204, 74-93 (2016a).

Kordy, M.A., Wannamaker, P.E., Maris V., Cherkaev, E., and Hill, G.J.: Three-dimensional magnetotelluric inversion using deformed hexahedral edge finite elements and direct solvers parallelized on SMP computers, Part II: direct data-space inverse solution: Geophysical Journal International, 204, 94-110 (2016b).

Miller, J.J., Allis, R. and Hardwick, C.: Seismic reflection profiling at the FORGE Utah EGS Site, *Geothermal Resources Council Transactions*, 42, 13 pp. (2018).

Miller, J., Allis, R., and Hardwick, C.: Interpretation of seismic reflection surveys near the FORGE enhanced geothermal systems site, Utah, *in* Allis, R., and Moore, J.N., editors, Geothermal characteristics of the Roosevelt Hot Springs system and adjacent FORGE EGS site, Milford, Utah: Utah *Geological Survey Miscellaneous Publication*, 169-H, 13 pp. (2019).

Miller, J.: 2018-2019 reprocessing of the 2D and 3D multichannel seismic surveys at the FORGE Utah EGS laboratory, *Utah FORGE Miscellaneous Report*, 34 pp. (2019).

Moore, J., McLennan, J., Allis, R., Pankow, K., Simmons, S., Podgorney, R., Wannamaker, P., Bartley, J., Jones, C., and Rickard, W.: The Utah Frontier Observatory for Research in Geothermal Energy (FORGE): An international laboratory for Enhanced Geothermal System technology development, *Proceedings*, 44th Workshop on Geothermal Reservoir Engineering Stanford University, Stanford, CA, SGP-TR-214, 12 pp. (2019).

Moore, J., McLennan, K., Pankow, K., Podgorney, R., Simmons, S., Wannamaker, P., Jones, C., Richard, W., Barker, B., Hardwick, C., and Kirby, S.: Overview of Utah Forge results in 2019, *Proceedings*, 45th Workshop on Geothermal Reservoir Engineering Stanford University, Stanford, CA, this issue, (2020).

Pankow, K., Mesimeri M., McLennan, J., and Moore, J.: Seismic monitoring at the Utah Frontier Observatory for Research in Geothermal Energy, *Proceedings*, 45th Workshop on Geothermal Reservoir Engineering Stanford University, Stanford, CA, this issue, (2020).

Pitz, W. and Miller, D.: The TerraSAR-X Satellite, *IEEE Transactions on Geoscience and Remote Sensing*, 48, 615-622, http://dx.doi.org/10.1109/TGRS.2009.2037432 (2010).

Sandwell, D., Mellors, R., Tong, X., Wei, M., and Wessel, P.: Open radar interferometry software for mapping surface deformation, *EOS*, Transactions American Geophysical Union, 92, 234-234 (2011).

Simmons, S.F., Kirby, S., Bartley, R., Allis, A., Kleber, E., Knudsen, T., Miller, J.J., Hardwick, C., Rahilly, K., Fischer, T., Jones, C., and Moore, J.: Update on the geoscientific understanding of the Utah FORGE site, *Proceedings*, 44th Workshop on Geothermal Reservoir Engineering Stanford University, Stanford, CA, SGP-TR-214, 10 pp. (2019).

Simmons, S., Allis, R., Kirby, S., Moore, J..: Production chemistry evidence for an EGS type reservoir in Roosevelt Hot Springs and implications for Utah FORGE, *Proceedings*, 45th Workshop on Geothermal Reservoir Engineering Stanford University, Stanford, CA, this issue, (2020).

Wannamaker, P., Rose, P., Doerner, W., Berard, B., McCulloch, J., and Nurse, K.: Magnetotelluric surveying and monitoring at the Coso geothermal area, California, in support of the Enhanced Geothermal Systems concept: survey parameters, initial results, *Proceedings*, 29th Workshop on Geothermal Reservoir Engineering, Stanford, CA, SGP-TR-175, 8 pp. (2004).

Wannamaker, P.E., Moore, J.N., Pankow, K.L., Simmons, S.F., Nash, G.D., Maris, V., Trow, A., and Hardwick, C. L.: Phase II of Play Fairway Analysis for the Eastern Great Basin extensional regime, Utah: status of indications, *Geothermal Resources Council Transactions*, 41, 2368-2382 (2017).

Wannamaker, P.E., Faulds, J.E., Kennedy, B.M., Maris, V., Siler, D.L., Ulrich, C., and Moore, J.N.: Integrating magnetotellurics, soil gas geochemistry and structural analysis to identify hidden, high enthalpy, extensional geothermal systems, *Proceedings*, 43rd Workshop Geothermal Reservoir Engineering, Stanford University, Stanford, CA, SGP-TR-214, 19 pp. (2019).

Witter, J.: 3D Geophysical modelling of gravity data at the Utah FORGE site, Innovate Geothermal Ltd., *Utah Geological Survey Miscellaneous Report*, project #0011, 24 pp. (2019).

Yilmaz, O.: Seismic Data Analysis: Processing, inversion, and interpretation of seismic data, *Society of Exploration Geophysics report*, 2065 p., http://dx.doi.org/10.1190/1.9781560801580. (2001).